Raman scattering boson peak and differential scanning calorimetry studies of the glass transition in tellurium–zinc oxide glasses

2010 J. Phys.: Condens. Matter 22 195103

(http://iopscience.iop.org/0953-8984/22/19/195103)

J. Phys.: Condens. Matter **22** (2010) 195103 (10pp) doi:10.1088/0953-8984/22/19/195103

Raman scattering boson peak and differential scanning calorimetry studies of the glass transition in tellurium–zinc oxide glasses

E Stavrou[1], C Tsiantos[1], R D Tsopouridou[1], S Kripotou[1], A G Kontos[1,2], C Raptis[1], B Capoen[3], M Bouazaoui[3], S Turrell[4] and S Khatir[4]

[1] Department of Physics, National Technical University of Athens, GR-15780 Athens, Greece
[2] Institute of Physical Chemistry, NCSR Demokritos, GR-15310 Athens, Greece
[3] Laboratoire de Physique des Lasers, Atomes et Molécules (CNRS, UMR 8523), Bâtiment P-5, Centre d'Etudes et de Recherches Lasers et Applications (CERLA-FR CNRS 2416), Université de Sciences et Technologies de Lille, F-59655 Villeneuve d'Ascq Cedex, France
[4] Laboratoire de Spectrochimie Infrarouge et Raman (CNRS 8516), Bâtiment C-5, Centre d'Etudes et de Recherches Lasers et Applications (CERLA-FR CNRS 2416), Université de Sciences et Technologies de Lille, F-59655 Villeneuve d'Ascq Cedex, France

E-mail: craptis@central.ntua.gr

Received 17 November 2009, in final form 26 February 2010
Published 16 April 2010
Online at stacks.iop.org/JPhysCM/22/195103

Abstract

Raman scattering and differential scanning calorimetry (DSC) measurements have been carried out on four mixed tellurium–zinc oxide $(TeO_2)_{1-x}(ZnO)_x$ ($x = 0.1, 0.2, 0.3, 0.4$) glasses under variable temperature, with particular attention being given to the respective glass transition region. From the DSC measurements, the glass transition temperature T_g has been determined for each glass, showing a monotonous decrease of T_g with increasing ZnO content. The Raman study is focused on the low-frequency band of the glasses, the so-called boson peak (BP), whose frequency undergoes an abrupt decrease at a temperature T_d very close to the respective T_g values obtained by DSC. These results show that the BP is highly sensitive to dynamical effects over the glass transition and provides a means for an equally reliable (to DSC) determination of T_g in tellurite glasses and other network glasses. The discontinuous temperature dependence of the BP frequency at the glass transition, along with the absence of such a behaviour by the high-frequency Raman bands (due to local atomic vibrations), indicates that marked changes of the medium range order (MRO) occur at T_g and confirms the correlation between the BP and the MRO of glasses.

(Some figures in this article are in colour only in the electronic version)

1. Introduction

Two major issues in condensed matter physics related to the dynamics of glass-forming systems, namely the glass transition and the low-frequency vibrational spectrum (measured in Raman scattering or neutron diffraction experiments) remain still controversial and largely unanswered considering the diversity with which these phenomena are manifested among various such systems (molecular or network glasses, fragile or strong ones). Regarding the nature of the glass transition [1], the debate is whether kinetic or thermodynamic aspects dominate and drive the transition from glass to supercooled liquid (and back). It is noteworthy that, while kinetic properties (diffusion, viscosity) sustain steep changes across the glass transition, thermodynamic quantities of the systems, such as volume and entropy, vary continuously at the transition. Some studies [2–4] have correlated the kinetic changes with thermodynamic ones over the glass transition, while others [5–7] have contested such correlations.

The glass transition and, generally, the dynamics of network glasses can be investigated by either relaxational (diffusion-like) [8–14] or vibrational [8–12, 15, 16] processes occurring at short and intermediate spatial scales of the glass. In low-frequency light scattering experiments, the relaxational processes give rise to the so-called quasi-elastic scattering, a central component which decays rapidly with frequency, but increases sharply in intensity as the glass transition temperature T_g is approached [8–14]. The non-central vibrational (Raman) component, that is, the broad asymmetric boson peak (BP), is still a matter of controversy and debate about its origin. The two components often overlap [8–12, 16, 17] in the frequency domain to an extent depending on the glass and temperature. However, in 'strong glasses', scattering in the region of the BP ($\omega \geqslant 10$ cm^{-1}) is dominated by vibrational rather than relaxational processes [8, 9, 16, 17].

It is broadly accepted that the BP represents an excess vibrational density of states of the glass, above the Debye level of the corresponding crystal. Although there have been many relevant experimental and theoretical studies over the past three decades, the scattering mechanism responsible for the BP remains still controversial. All current theories [18–21] consider that additional non-Debye vibrational modes interact (hybridize) with Debye acoustic phonons to give the BP profile. The first of these theories is based on the soft potential model [18] and relates the BP to weakly interacting quasilocal harmonic oscillations whose interaction increases with energy. When the medium becomes vibrationally unstable, due to an increased level of interaction, the model [18] incorporates also anharmonic contributions. In other recent studies [19–21], the BP has been attributed to hybridization of Debye acoustic modes with short wavelength acoustic- or optic-like modes [19], localized optic modes of nanoscale heterogeneities [20] or defect harmonic modes arising from randomly fluctuating elastic disorder and specifically from spatially fluctuating elasto-optic constants of the medium [21]. In spite of the different assumptions and approaches, all current theories [18–21] agree with the concept that additional, non-Debye, modes contribute to the scattering of the BP in glasses.

The boson peak has been associated in the past by several authors [22–27] with the medium range order (MRO) of glasses correlating the BP frequency to a mean size of the MRO [23]. In recent years, references on the BP–MRO correlation have become less frequent and current theories bypass, on the whole, this aspect. However, whatever the objections are about the existence of this correlation, it is broadly accepted that the BP is related to vibrational processes beyond the atomic scale of glasses.

It is generally known that the high-frequency bands of the Raman spectrum of glasses are not significantly influenced by the drastic dynamic effects occurring over the glass transition and the variation of their frequency at T_g follows a normal thermal softening dependence. This indicates that the atomic structure remains, by and large, unaffected across the glass transition, in spite of a change of viscosity by many orders of magnitude. However, in certain cases involving fragile glasses [28, 29], some spectral characteristics of these bands have displayed small, but not steep, changes at T_g. In contrast, there have been indications in several categories of glasses [8–10] that the BP softens at T_g at a rate much higher than that anticipated by the thermal softening. Nevertheless, the softening of the BP at T_g has not been investigated systematically in any glassy system. In the past, based on inelastic neutron scattering measurements [15], the vibrational density of states of glassy and supercooled liquid selenium was determined, showing a large increase of the latter (relative to the former) in the low-frequency region, that is, in the BP region. It must be pointed out, though, that the relevant densities of states of the two phases [15] did not refer to temperatures across the glass transition, but at temperatures very distant from T_g (200 and 160 K below and above T_g, respectively). Since that report [15], there have been no other relevant studies over the glass transition. Therefore, knowledge of the low-frequency vibrational dynamics of glasses in the vicinity of T_g is rather limited.

Recent Raman studies [30, 31] of chalcogenide glasses at high temperatures have shown that certain BP spectral characteristics (frequency and intensity) are very sensitive to dynamical effects over the glass transition sustaining abrupt changes as T_g is approached. Because of these findings, it has been suggested [30, 31] that low-frequency Raman scattering can be used as a technique complementary to calorimetry for an approximate determination of T_g in glasses.

In this work, we report the results of combined Raman spectroscopic and differential scanning calorimetry (DSC) studies of the glass transition in oxide glasses and specifically in four tellurium–zinc oxide $(TeO_2)_{1-x}(ZnO)_x$ ($x = 0.1$, 0.2, 0.3, 0.4) glasses. Both the high-frequency atomic vibrations spectrum and the boson peak are studied under variable temperature from 24 K up to crystallization. Bearing in mind the previous relevant Raman studies on chalcogenide glasses [30, 31], it is challenging to find out whether Raman scattering, and especially the BP component, can be reliably used also in the case of oxide glasses for the determination of T_g and for the study of the glass transition as a whole. Two sets of T_g values have been obtained (from Raman and DSC measurements) and found to be in very good agreement with each other. As analysis of the Raman data has progressed, it has become clear, for all glasses, that the temperature dependence of the BP around T_g is drastically different from that of any high-frequency bands of the spectrum, showing that marked changes in the medium range order occur at T_g and confirming a definite BP–MRO correlation in these glasses.

2. Structure of mixed $(TeO_2)_{1-x}(ZnO)_x$ glasses

Tellurium oxide (TeO_2) is a polymorphous material appearing in several crystalline phases at ambient conditions with rather complicated, but compact structures [32, 33]. Pure TeO_2 forms rather unstable glassy phases, but when mixed with metal oxide modifiers [34–42], such as alkali metal M_2O (M = Li, Na, K, Rb, Cs) [34–36] or other metal MO (M = Mg, Sr, Ba, Zn, Pb) [37–42] oxides, stable network glasses can be obtained over wide composition ranges with interesting properties, the most notable of which is their good optical

transmittance [38, 40] in the visible and near-infrared parts of the spectrum. This property makes them suitable host materials for rare-earth cations and the development of optical amplifiers in the near-infrared [43, 44]. The structure of mixed tellurite glasses has been investigated by neutron diffraction [34, 39, 40], Raman [35, 37, 40–42], IR [38, 40] and NMR [36] spectroscopies.

When the modifier is ZnO, stable $(TeO_2)_{1-x}(ZnO)_x$ glasses are formed over the range: $0.05 \leqslant x \leqslant 0.45$ [45]. Various reports [34, 39–42] have suggested that the atomic structure of these tellurite glasses resembles closely that of the paratellurite (α-TeO_2) crystalline phase [32, 33] which displays a three-dimensional crystalline lattice of TeO_4 trigonal bipyramids. In each TeO_4 unit, two axial Te–O_{ax} bonds are oriented at almost opposite directions, while the other two equatorial Te–O_{eq} ones are at a smaller angle between them and lie in a plane perpendicular to the direction O_{ax}–Te–O_{ax} [32, 33]. Raman data of pure TeO_2 glass [32, 33] indicate that the three-dimensional glassy network is built up by deformed TeO_4 bipyramids. The introduction of ZnO strengthens this network and results in a gradual modification of TeO_4 bipyramids first to TeO_{3+1} and then to TeO_3 polyhedra whose population increases with increasing ZnO content [34, 39–42]. For low ZnO concentrations, some bipyramids become asymmetrical with one axial Te–O_{ax} bond being elongated and the other shortened, thus producing TeO_{3+1} polyhedra. As the ZnO content is increased, several TeO_{3+1} polyhedra gradually loose the oxygen atom in the elongated bond and evolve to (strongly bound) trigonal TeO_3 pyramids in which one of the remaining oxygen atoms forms a terminal double Te=O bond [34, 36]. In a neutron diffraction study [39], it has been suggested that ZnO is incorporated in the glassy network in the form of bridging ZnO_6 octahedra with corner sharing axial and equatorial oxygen atoms of the TeO_4, TeO_{3+1} and TeO_3 units. However, there are no further reports that the ZnO modifier participates in the glassy network. Instead, other neutron diffraction [34, 40] and Raman [35, 40–42] studies have implied that the network of $(TeO_2)_{1-x}(ZnO)_x$ glasses is dominated by deformed (asymmetrical) TeO_4 bipyramids.

3. Experimental and data analysis procedures

Glassy $(TeO_2)_{1-x}(ZnO)_x$ samples were prepared by quenching the melts; details on the preparation of glasses are given in [42]. The Raman spectra were excited by the 514.5 nm line of an Ar^+ laser at a power of ~200 mW measured just before the cryostat or the furnace, using a nearly backscattering geometry. Polarized HH and VH Raman spectra were recorded, with parallel- and cross-polarizations of incident/scattered light, respectively. The VH component displayed better resolution of the BP and was preferred for the study of this band, especially at high temperatures where the level of quasi-elastic scattering became appreciable. On the other hand, the HH component gave a much stronger high-frequency spectrum and, for this reason, it was used for the study of the corresponding Raman bands.

The low temperature experiments were performed using a closed cycle He optical cryostat (20–300 K), while the high temperature ones inside an optical furnace (300–1200 K) of very low temperature gradients. A large number of data points were obtained under variable temperature particularly in the vicinity of the (previously determined by calorimetry) T_g, where the step of temperature increment was as low as 3 K. Scattered light was first analysed by a SPEX 1403 double spectrometer and then detected by a cooled photomultiplier.

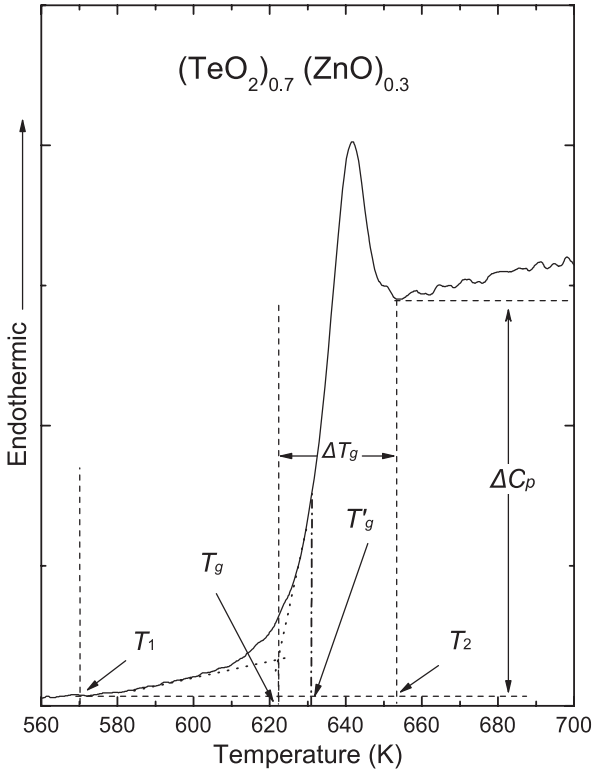

Figure 1. Differential scanning calorimetry (DSC) thermogram of the $(TeO_2)_{0.7}(ZnO)_{0.3}$ glass in the region 560–700 K, showing the two slightly different ways of defining the glass transition temperature. T_1, T_2: onset and completion points of the endothermic process. ΔT_g: width of the glass transition region.

The fitting procedures used for the evaluation of Raman band frequencies, and in particular those for the frequency of the broad, asymmetric BP profile, have been described in previous relevant publications [17, 30, 31]. Furthermore, in the present work we have performed additional tests to assess the extent of overlapping between the high-frequency tail of the quasi-elastic scattering and the BP, and find out whether it affects the determination of the BP frequency. The procedures and results of these tests are presented and discussed in section 4.

A heat flux differential scanning calorimeter was used at a heating rate of 10 K min^{-1} in nitrogen atmosphere. Details about the determination of T_g from the DSC measurements are given in section 4.

4. Results

A typical DSC thermogram is shown in figure 1 for the $(TeO_2)_{0.7}(ZnO)_{0.3}$ glass in the region 560–700 K. From such thermograms, two different approaches have been applied for

Table 1. Boson peak frequencies ω_{bos}, glass transition temperatures T_g and T'_g, width of the glass transition region ΔT_g and critical temperatures T_d and T_f of the four $(TeO_2)_{1-x}(ZnO)_x$ glasses obtained from the Raman data; all values are from this work, except the T_g ones determined from differential thermal analysis (DTA) data[a].

Glass (x)	ω_{bos} (300 K) (cm^{-1})	T_g (DSC) (K)	T'_g (DSC) (K)	ΔT_g (DSC) (K)	T_g (DTA) (K)	T_d (Raman) (K)	T_f (Raman) (K)
0.1	41 ± 3	658 ± 4	660 ± 2	30 ± 5	590[a]	660 ± 5	720 ± 10
0.2	40	644	646	37	597[a]	648	694
0.3	41	622	630	35	601[a]	618	710
0.4	43	620	628	30		620	704

[a] Reference [37].

the evaluation of T_g, giving slightly different values: in the first one, used also in previous studies [46, 47], the T_g values can be obtained by the crossing of two linear extrapolations on either side of the DSC curve ascent (see figure 1). Alternatively, in the second approach, slightly higher T'_g values have been determined by considering as the glass transition temperature the point at which the specific heat rises to a value $\Delta C_p/2$, where ΔC_p is the total specific heat variation over the entire temperature range corresponding to the endothermic process associated with the transition to the supercooled phase. The temperature in which the slope of the DSC curve starts increasing ($T_1 \approx 570$ K for the glass of figure 1) is taken as starting point T_1 for the endothermic process. Completion of the transition is denoted at the point T_2 where the DSC curve reassumes almost linear dependence with temperature ($T_2 \approx 653$ K in figure 1). The quantity $\Delta T_g = T_2 - T_g$, known [46, 47] as the width of the glass transition region, is a measure of the temperature range associated with the endothermic process and has been related with the viscosity [46] and the strong/fragile character of glasses [47]. It is generally accepted that the larger the ΔT_g, the stronger the glass. Values of T_g, T'_g and ΔT_g for the four glasses of this study obtained by DSC measurements are shown in table 1. Also, in table 1, T_g values are given (for only three of the four glasses) from a previous work [48] in which the differential thermal analysis (DTA) method has been used. Furthermore, table 1 also contains the BP frequencies ω_{bos} (at 300 K), and characteristic temperatures T_d and T_f as determined from the BP and generally the Raman spectra (see below in this section and in section 5.3).

The ambient conditions HH Raman spectra of the four $(TeO_2)_{1-x}(ZnO)_x$ glasses covering the entire frequency range are given in figure 2. Separate VH spectra (favouring depolarized scattering) of the glasses in the low-frequency region (5–250 cm^{-1}) plotted in linear-log scales are shown in figure 3, giving in detail the BP profiles. Based on such linear-log profiles, we have determined the frequency ω_{bos} of the BP (for details, see [17]). The high-frequency spectrum consists of two broad features in the regions 290–550 cm^{-1} and 600–900 cm^{-1}. The peak position of the former feature varies monotonously with composition ranging from 442 ($x = 0.1$) to 410 cm^{-1} ($x = 0.4$), while the latter displays two definite peaks at about 670 and 755 cm^{-1}. In a previous Raman study [41] of mixed MO–TeO_2 glasses, scattering in the 600–900 cm^{-1} region was deconvoluted to four components. In the absence of clear spectral evidence and bearing in mind the complexity of the structure (which makes it difficult to predict the multiplicity of the expected normal vibrations), such a multicomponent deconvolution may have no physical significance. We have attempted to fit in this spectral region to two bands corresponding to the two spectrally resolved peaks, but without much success. This failure is attributed to an apparent shoulder which is evident on the high-frequency side. Instead, we have successfully fitted this region to three bands and the result of this fitting for the $x = 0.4$ glass is shown in the inset of figure 2, giving peaks at about 670, 750 and 790 cm^{-1}. Further comments justifying the choice of three component fitting are given in section 5.2.

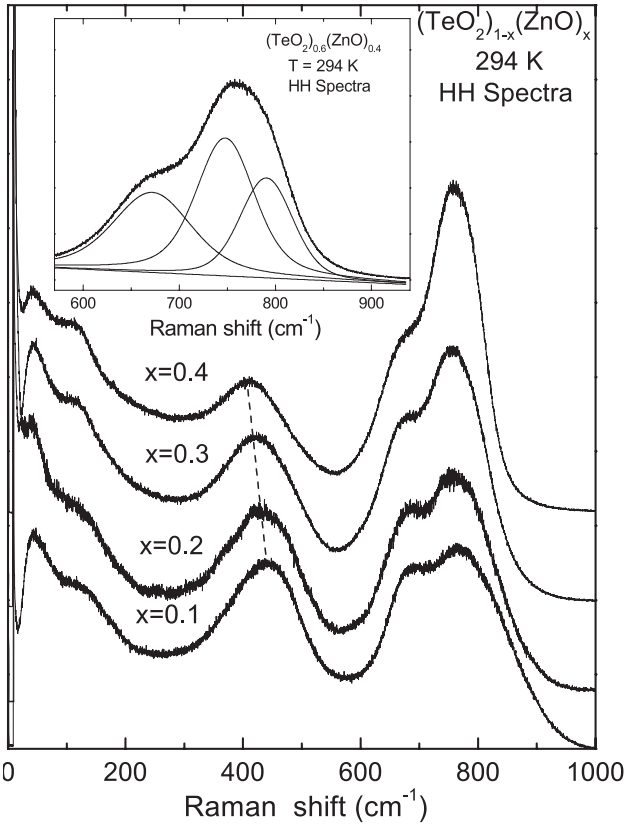

Figure 2. Raman spectra for the four $(TeO_2)_{1-x}(ZnO)_x$ glasses at ambient conditions; the inset shows the Raman scattering for the $(TeO_2)_{0.6}(ZnO)_{0.4}$ glass in the high-frequency region (570–900 cm^{-1}) fitted to three peaks.

The evolution of the HH Raman spectrum of the $(TeO_2)_{0.7}(ZnO)_{0.3}$ glass with increasing temperature is shown in figure 4. The temperature range starts at 20 K, covers the glass transition and spans up to complete crystallization of the

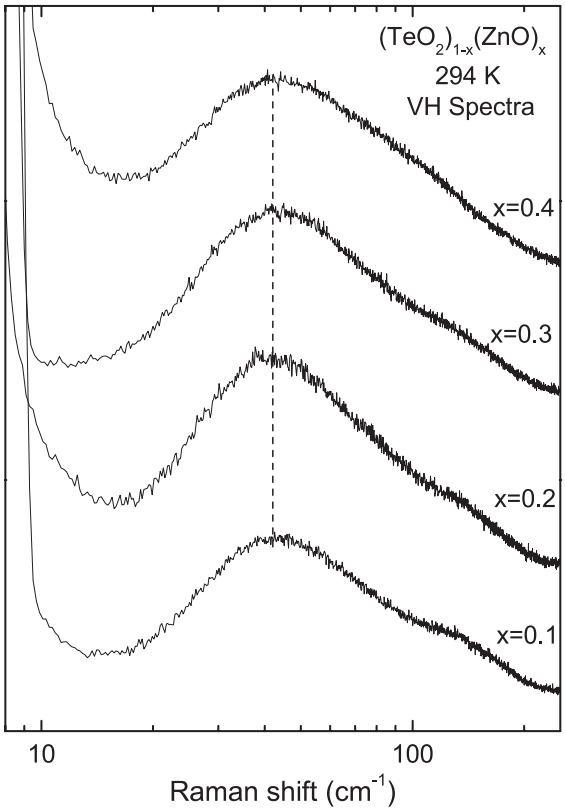

Figure 3. Low-frequency Raman spectra for the four $(TeO_2)_{1-x}(ZnO)_x$ glasses at ambient conditions plotted in linear-log scales, showing in detail the Boson peak profile.

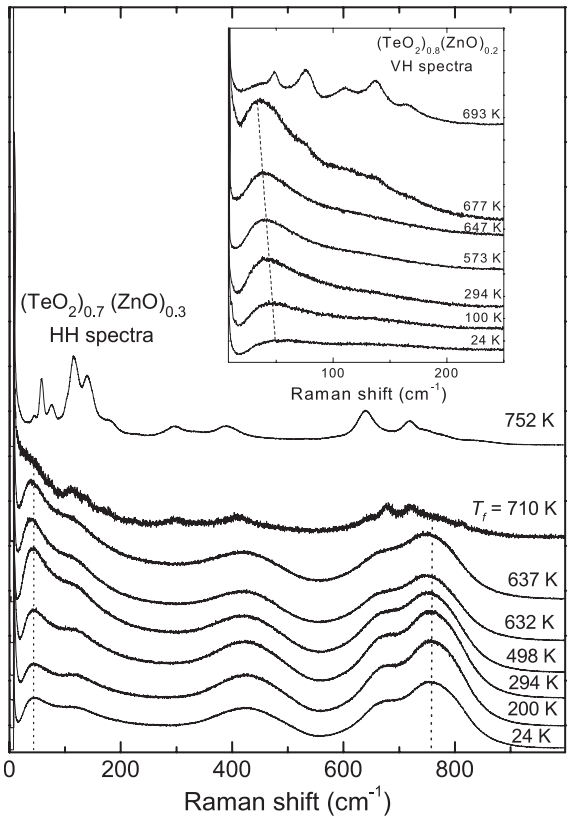

Figure 4. Polarized HH Raman spectra of the $(TeO_2)_{0.7}(ZnO)_{0.3}$ glass at various temperatures from 24 K, through the glass transition and up to crystallization. The inset shows the evolution of the boson peak of the $(TeO_2)_{0.8}(ZnO)_{0.2}$ glass with increasing temperature.

glass (upper spectrum at 752 K). The onset of crystallization (T_f = 710 K) is assumed to occur when the high-frequency, atomic vibrations bands start becoming sharp and the BP disappears. The inset of figure 4 shows the evolution with temperature of the BP profile for the $(TeO_2)_{0.8}(ZnO)_{0.2}$ glass. Similar qualitative temperature evolutions of spectra have been displayed by the other glasses, with some variations among them due to different characteristic temperatures.

Plots giving the temperature dependence of the BP frequency ω_{bos} of the glasses are shown in figures 5 (x = 0.1, 0.2) and 6 (x = 0.3, 0.4). For comparison, in the insets of figures 5 and 6, additional ω_{hf}–T plots are given for the high-frequency band at 750 cm^{-1} for the x = 0.2 and 0.3 glasses. An abrupt drop of the BP frequency takes place at a temperature T_d (figures 5 and 6) which varies from one glass to the other. The measured values of characteristic T_d and T_f temperatures are given in table 1.

Although the BP is clearly resolved up to the highest temperature of its detection (figure 4 and inset), to find out whether the determination of the ω_{bos} frequency of the BP is influenced by the quasi-elastic (and elastic) scattering component, we have fitted the latter component to a power-law function (as in a recent study of the quasi-elastic scattering in polymer glasses [49]), extrapolated for $\omega > 15$ cm^{-1} and subtracted it from the respective recorded spectrum. We have performed these subtraction procedures for all glasses and all temperatures recorded, and found that the quasi-elastic scattering (QES) interference in the estimation of ω_{bos} is either marginal or negligible. Given that around T_g the QES becomes very strong [8–14] and the BP is downshifted relative to its ambient condition position, the overlapping between the two scattering components is expected to be deeper in this temperature region than in any other. Figure 7 shows the low-frequency scattering from the four glasses (at temperatures above the respective T_g values) plotted in log–log scales, the QES fittings and the resultant spectra after subtraction of the QES. Only in the case of the x = 0.3 glass (figure 7(c)) do the ω_{bos} values determined with and without QES subtraction differ, but only marginally. We have reproduced the ω_{bos}–T plot (figure 8) for this glass including the ω_{bos} values after QES subtraction. It is evident that, even after QES subtraction, the corrected ω_{bos} values also display a steep drop as the glass approaches and goes over T_g. Finally, the inset of figure 8 shows a plot of ω_{min} against temperature, where ω_{min} is the frequency corresponding to the 'dip' between the QES and BP (see also figure 7). It is apparent from this plot that ω_{min} increases sharply as T_g is approached. Correlation of this plot with the ω_{bos}–T plots (figures 5 and 6 and the main frame of figure 8) is discussed in section 5.3.

5. Discussion

5.1. DSC measurements

The two sets of T_g and T_g' values determined in this work by the two procedures of DSC data analysis are very close,

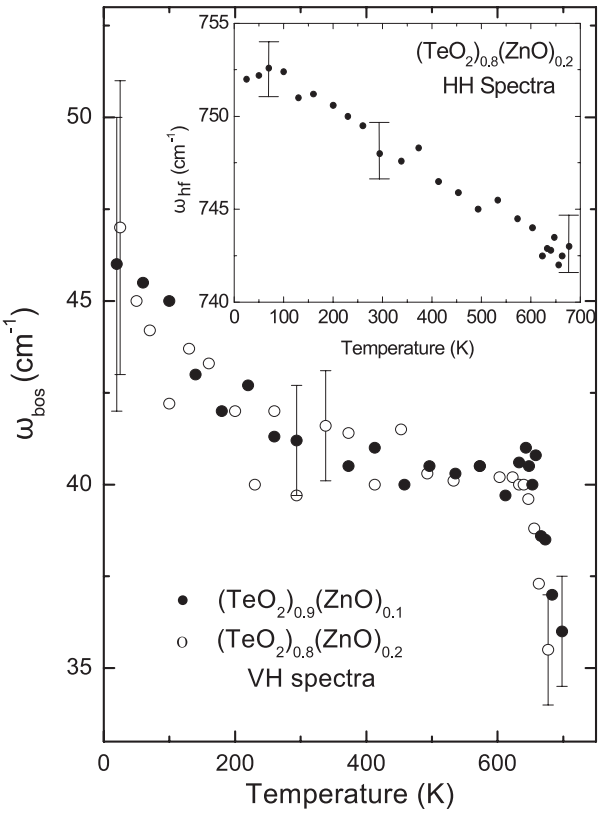

Figure 5. Boson peak frequency ω_{bos} plots as a function of temperature for the $(TeO_2)_{0.9}(ZnO)_{0.1}$ and $(TeO_2)_{0.8}(ZnO)_{0.2}$ glasses. The inset shows the respective plot for the high-frequency molecular band at 750 cm^{-1} of the latter glass.

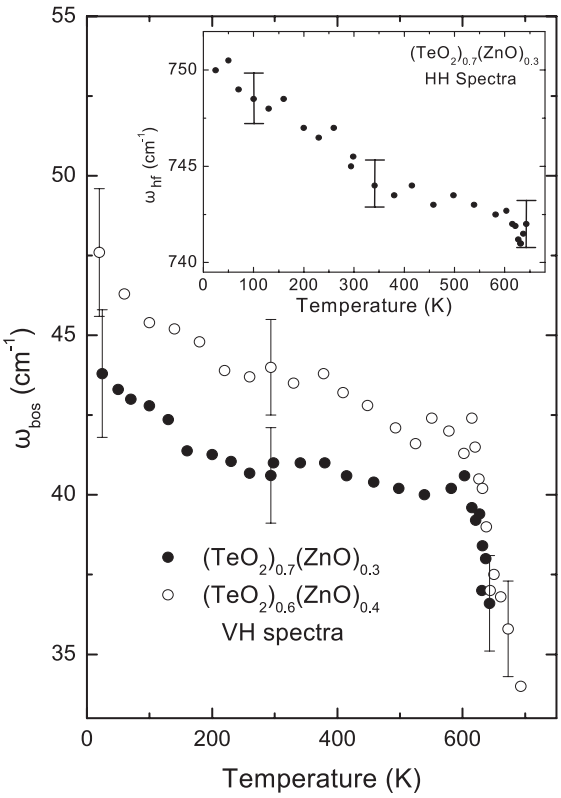

Figure 6. Boson peak frequency ω_{bos} plots as a function of temperature for the $(TeO_2)_{0.7}(ZnO)_{0.3}$ and $(TeO_2)_{0.6}(ZnO)_{0.4}$ glasses. The inset shows the respective plot for the high-frequency molecular band at 750 cm^{-1} of the former glass.

with $T_g < T_g'$ (figure 1, table 1). From now on, in line with other authors [46, 47], all DSC glass transition temperatures measured in this work will refer to the set of T_g values obtained by the crossing of the two linear extrapolations of the thermogram curve ascent (figure 1). These values are significantly higher than the T_g values obtained by DTA data [48]. This discrepancy can be partially attributed to the different experimental techniques (DSC and DTA) and the conditions of preparation of glasses. However, we think that the differences in T_g values are primarily due to different definitions of the glass transition temperature. Hence, it appears that the authors of [48] consider as T_g the point at which the endothermic process begins, while we, as well as other authors [46, 47], adopt an advanced (mid-point) stage of this process.

The glass transition temperature of a pure TeO_2 glass was measured a long time ago using the DSC technique [50] and found to be $T_g = 593$ K, a value which is quite low compared to those of the mixed tellurite glasses of this work for which T_g decreases with increasing ZnO concentration (table 1). It appears that, after its initial stabilizing influence at low concentrations, the ZnO modifier has an adverse effect on T_g. This effect is largely anticipated as further ZnO doping is expected to reduce the connectivity of glasses because of interruptions of the continuous network of TeO_4 bipyramids which results in a continuously increasing number of terminal Te=O bonds (in TeO_3 polyhedra). The four glasses of this study display rather large and comparable ΔT_g temperature widths for their glass transitions (table 1). According to an empirical criterion [47], glasses displaying widths $\Delta T_g \geqslant 30$ K are classified as 'strong' and, therefore, considering the ΔT_g values observed here, the mixed tellurium–zinc oxide glasses can be characterized, on the whole, as strong ones.

5.2. Raman spectra at ambient conditions

Prior to discussing the Raman data over the glass transition, it is instructive to review the assignments of the Raman bands of the glasses at ambient conditions as are deduced from the comparison of previous relevant studies and the spectra of this work.

The ambient condition Raman spectra of the mixed $(TeO_2)_{1-x}(ZnO)_x$ glasses of this work (figure 2) are in very good agreement with those of previous studies [41, 42]. A well-resolved BP is displayed by all glasses in the VH configuration at a frequency $\omega_{bos} \approx 40$ cm^{-1} (figure 3, table 1). The broad band (shoulder) centred around 130 cm^{-1} is more pronounced in the HH component (figure 2) and can be considered as residuals of low-frequency optic modes of the crystal as the Raman spectrum of the α-TeO_2 paratellurite crystalline phase [32, 33] displays strong optical phonon bands in the low-frequency region. This idea is confirmed in the present study by the observation in this region of strong and well-resolved bands in the spectrum of the crystallized materials above T_g (figure 4).

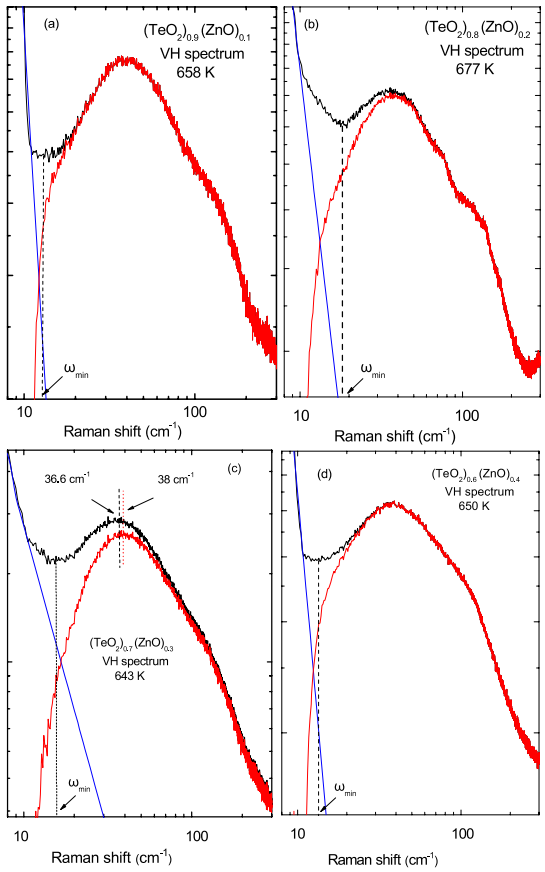

Figure 7. The low-frequency light scattering spectra for the four $(TeO_2)_{1-x}(ZnO)_x$ glasses plotted in log–log scales, showing the quasi-elastic and the boson peak (Raman) components. The spectra were recorded at a temperature above the respective glass transition temperatures T_g. The quasi-elastic component has been fitted to a power-law function and then extrapolated for $\omega > 15$ cm^{-1}. Subtraction of the quasi-elastic component from the recorded spectrum gives the net scattering of the vibrational (BP) component. ω_{min} is the (frequency) position of the 'dip' in between the two scattering components (see the text for details).

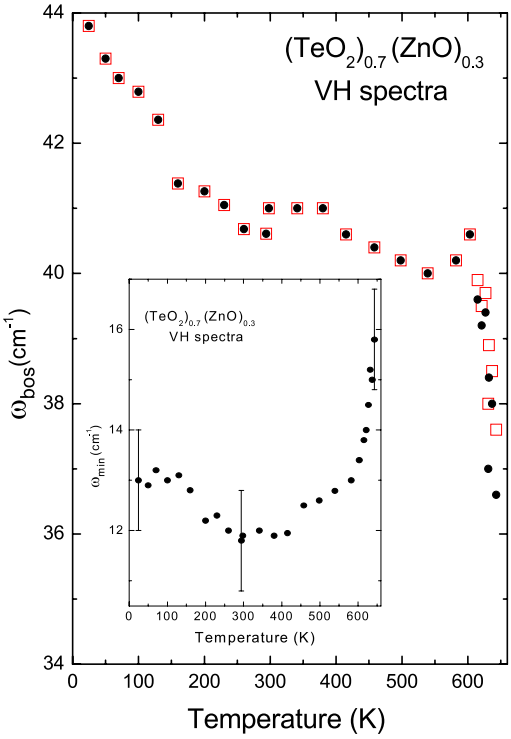

Figure 8. Boson peak frequency ω_{bos} plots as a function of temperature for the $(TeO_2)_{0.7}(ZnO)_{0.3}$ glass with (full symbols) and without (open symbols) subtraction of the quasi-elastic scattering component. The inset shows a plot of the frequency ω_{min} as a function of temperature for the $(TeO_2)_{0.7}(ZnO)_{0.3}$ glass, where ω_{min} is the position of the 'dip' in between the quasi-elastic and boson peak scattering components (see the text for details).

The peak position and intensity of the mid-frequency band depend on ZnO concentration (figure 2). This band is observed in the Raman spectrum of pure TeO_2 glass at 450 cm^{-1} [32, 33] and has been assigned [41, 42] to bending vibrations of Te–O–Te bridges which are formed by vertex-sharing linkages of TeO_4 bipyramids, and TeO_{3+1} and TeO_3 polyhedra. This band decreases in intensity and downshifts continuously from about 440 ($x = 0.1$) to 410 cm^{-1} ($x = 0.4$), thus implying that the modifier reduces the hardness of the relevant bonds and the rigidity of the glassy network. The reduction in intensity reflects the decrease in the number of Te–O–Te units.

As mentioned in section 4, we have fitted the spectral region between 600 and 900 cm^{-1} to three bands, with two of them close to the observed peaks and the third at the high-frequency shoulder (see the inset of figure 2). The position of the lower-frequency band at about 670 cm^{-1} has been found [42] to be virtually independent of the metal oxide MO modifier. In the Raman spectrum of the pure TeO_2 glass, this band is the strongest feature [32, 33]. From our spectra (figure 2), it is evident that the position of this band is almost independent of the amount of ZnO modifier. Hence, this band at 670 cm^{-1} should be attributed to the backbone of the TeO_2 glassy network and more specifically to stretching vibrations in deformed TeO_4 bipyramids.

The intensity of the next band at 750 cm^{-1} increases strongly with ZnO content (figure 2), while its position has been found [42] to depend monotonically on the MO modifier. This band is practically absent in the spectrum of pure TeO_2 glass [32, 33]. Therefore, it is reasonable to attribute it primarily to stretching modes in TeO_{3+1} and TeO_3 groups [42]. As has been pointed out in [42], the ratio of intensities of the bands at 670 and 750 cm^{-1} can be taken as a measure of the relative population of TeO_4 bipyramids against the TeO_{3+1} and TeO_3 polyhedra. Given the presence of the tight double Te=O bond in the TeO_3 unit, it is expected that the frequency of stretching vibrations in this unit will be higher than that in the TeO_4 and TeO_{3+1} units and this is actually the physical incentive for fitting the scattering in the 600–900 cm^{-1} region to three bands, giving the third peak at 790 cm^{-1}.

5.3. High temperature Raman measurements

It is evident from the spectra of figure 4 that both the BP and high-frequency bands downshift with increasing temperature and this is accompanied by a relative intensity increase of the BP with respect to that of the high-frequency bands. The

BP is clearly resolved above T_g up to a certain temperature, depending on the glass (figure 4). Finally, at a temperature T_f (≈710 K for the $x = 0.3$ glass, figure 4), the high-frequency Raman bands become sharp, implying the onset of crystallization, a process which is completed in this glass at about 750 K. At this temperature, all trace of the BP has vanished. The Raman spectrum of the material after crystallization is almost the same for all four compositions and similar to that of the paratellurite α-TeO_2 [32, 33]. Therefore, as has also been found previously [42], the crystallized material is that of TeO_2, irrespective of the type or concentration of the metal MO modifier. This result casts a doubt about the extent the ZnO modifier is incorporated in the glassy TeO_2 network, as has been claimed in [39].

Before discussing the frequency variation of the various Raman bands across the glass transition, we make some comments on the temperature dependence of the BP frequency ω_{bos} in the region from 24 K up to T_g. It appears from the main graphs of figures 5, 6 and 8 that ω_{bos} downshifts with increasing temperature at a higher rate in the region 24–200 K as compared to the region 200-T_g, so that the overall ω_{bos} variation resembles a three-stage behaviour. Apparently, this looks more pronounced for the low ZnO concentration glasses ($x = 0.1$ and 0.2). However, such three-stage behaviour is not real, but simply the determination of the peak position of the BP is significantly affected by the marked decrease of the BP intensity at low temperatures (figure 4). This intensity decrease is anticipated by the Bose–Einstein thermal factor for the low-frequency vibrational scattering at low temperatures, and in combination with the presence of the broad band at 130 cm^{-1} (whose intensity is not affected as much) results in an artificial additional upshift of ω_{bos}. Other side effects of the intensity variations of the two scattering components (BP and quasi-elastic scattering) at low frequencies are illustrated in the inset of figure 8 which shows the ω_{min}–T plot for the 'dip' between the quasi-elastic scattering and the low-energy side of the BP. At low temperatures, the low level of the BP results in an additional upshifting of the 'dip'. Then, as the BP intensity increases with increasing temperature, ω_{min} decreases, reaching a plateau which is followed by a sharp increase when T_g is approached because the quasi-elastic scattering becomes very strong. However, as seen from the corrected spectra of figure 7, the increased level of quasi-elastic scattering across the glass transition does not significantly affect the peak frequency ω_{bos} of the BP.

The ω_{bos}–T plots of figures 5, 6 and 8 display a sharp drop of BP frequency for all glasses at a temperature T_d which lies very close to the respective T_g determined by DSC (table 1). This steep softening indicates instability of the vibrational modes (and therefore the structure) associated with the BP. In contrast, the high-frequency band at 750 cm^{-1} (ω_{hf}–T plots in insets of figures 5 and 6) downshifts continuously (smoothly) with temperature over the entire range of study, thus displaying a normal thermal softening. Similar thermal softening has been observed for the other high-frequency bands of the four glasses. Hence, the abrupt dynamical effects occurring across the glass transition, which coincide with the BP frequency collapse, are not 'detected' by the local (atomic) order of the glasses and, therefore, should be related to instability of a domain well beyond the atomic distance scale. The contrasting temperature dependence of the BP and high-frequency bands over the glass transition is rather counteractive to hybridization theories about the origin of the BP which involve, apart from Debye-like acoustic waves, either short wavelength acoustic- or optic-like modes [19], or localized modes due to heterogeneities [20].

It is therefore evident that the abrupt drop of BP frequency at T_d (T_g) implies substantial changes in the medium range order. This steep decrease of ω_{bos} can be attributed to a significant reduction of cross-linking strength (decrease of force constants) between various structural units, and particularly TeO_{3+1} and TeO_3 polyhedra which tend to detach from the backbone network of TeO_4 bipyramids at high temperature. This decrease of MRO bonding strength may also involve small rearrangements of relative orientations of the structural units, but without altering the atomic coordination within the units. The proposed MRO changes are in line with the general notion of a transition from rigid glass to a more flexible material in the supercooled phase and the observation of an enormous change of viscosity at T_g [1, 3, 4]. Furthermore, the observed steep softening of the BP at T_g is expected to be accompanied by a downshift of the peak of the vibrational density of states and a large increase of the latter across the glass transition. Only one relevant experimental study has been reported in the past on glassy and supercooled Se [15] confirming such changes in the vibrational density of states. From that study [15], the relative contributions of the vibrational and relaxational processes to the excess entropy of the supercooled phase were also determined. The BP results of this work are compatible with several reports [4, 7, 15, 29] that the vibrational contribution to the excess entropy amounts to a high proportion (20–40%).

In contrast, it is evident for the present glasses that the atomic bonding strength within the various structural units does not sustain a discontinuous decrease at T_d (T_g) as the high-frequency bands downshift continuously with temperature across the glass transition (insets of figures 5 and 6) in a way anticipated by thermal softening. Small discontinuities of spectral characteristics of the high-frequency bands at T_g have been reported for polymer [28] and for sulfur-rich chalcogenide [29] glasses. However, these categories of glasses are on the fragile side of the fragile/strong division of glasses, while the tellurite glasses of the present work belong to the strong side of this division (see section 5.1 and [47]). Therefore, as T_d (T_g) is approached and passed, significant changes occur in the medium range order of these glasses which are not accompanied by similar changes in the atomic structure. Hence, the abrupt spectral changes of the BP around T_d (T_g) provide strong evidence that a correlation exists between BP and MRO in tellurite glasses.

Furthermore, the evolution with temperature of the Raman spectra of this work is compatible with the general idea that the BP becomes more pronounced and shifts to lower frequencies as the glass approaches instability [21]. A glassy system becomes unstable by either spatial (static) disorder, such as spatial fluctuation of elastic properties [21] and/or local

heterogeneities [20], or by dynamical disorder when the system approaches and goes through the glass transition.

It is remarkable that the two sets of T_g and T_d values for the tellurite glasses obtained by DSC and Raman (BP) measurements, respectively, are in very good agreement (table 1). These results are even better than those witnessed in chalcogenide glasses [30, 31]. Assuming DSC as the principal technique for the estimation of T_g, we conclude that accurate measurement and analysis of the boson peak over the glass transition region can provide equally reliable T_g values in the case of network glasses. Hence, low-frequency Raman scattering can be applied as a complementary (to DSC) technique for monitoring the glass transition and determining the T_g in such glasses.

6. Conclusions

The glass transition temperatures T_g of four tellurium–zinc oxide $(TeO_2)_{1-x}(ZnO)_x$ glasses have been determined by differential scanning calorimetry (DSC) measurements. Using two different approaches of DSC data analysis, two sets of very close values of T_g have been obtained. It is found that T_g decreases with increasing ZnO modifier concentration, implying (as anticipated) that the glassy network softens monotonically with ZnO doping.

From the Raman spectra of the glasses at ambient conditions it is concluded that the population of TeO_{3+1} and TeO_3 polyhedra increases with ZnO concentration at the expense of TeO_4 trigonal bipyramids which are the basic structural units of these glasses.

It has been found that the boson peak (BP) is critically affected by the dynamical effects occurring at the glass transition and, more specifically, that the BP frequency drops sharply as T_g is approached. On the other hand, the high-frequency Raman modes (due to atomic vibrations) do not display such a critical dependence. These bands soften continuously at and above T_g displaying an overall thermal softening dependence. These results imply that the short range order is practically unaffected by the drastic dynamical effects (indicated by the BP dependence) which take place at the glass transition. These contrasting results suggest that the glass transition in these glasses is associated with significant changes in the medium range order (MRO). It can also be deduced that a definite correlation exists between the BP and the MRO of glasses, a correlation which has been questioned during the past few years. Furthermore, the study of the BP at elevated temperatures, and in particular the abrupt drop of the BP frequency at the glass transition, can provide a reliable means for an estimation of T_g in network glasses which is an alternative to DSC.

Acknowledgments

The work was supported by the National Technical University of Athens (NTUA) in the framework of basic research program 'K Karatheodori' through grant 65/1601.

References

[1] Dyre J C 2006 *Rev. Mod. Phys.* **78** 953
[2] Speedy R J 1999 *J. Phys. Chem.* B **103** 4060
[3] Ito K, Moynihan C T and Angell C A 1999 *Nature* **398** 492
[4] Martinez L-M and Angell C A 2001 *Nature* **410** 663
[5] Roland C M, Santangelo P G and Ngai K L 1999 *J. Chem. Phys.* **111** 5593
[6] Ngai K L and Yamamuro O 1999 *J. Chem. Phys.* **111** 10403
[7] Johari G P 2002 *J. Chem. Phys.* **116** 2043
[8] Sokolov A P, Rössler E, Kisliuk A and Quitmann D 1993 *Phys. Rev. Lett.* **71** 2062
[9] Rössler E, Sokolov A P, Kisliuk A and Quitmann D 1994 *Phys. Rev.* B **49** 14967
[10] Brodin A, Börjesson L, Engberg D and Torell L M 1996 *Phys. Rev.* B **53** 11511
[11] Novikov V N 1998 *Phil. Mag.* B **77** 381
[12] Surovtsev N V, Pugatsev A M, Nenashev B N and Malinovsky V K 2003 *J. Phys.: Condens. Matter* **15** 7651
[13] Sokolov A P and Novikov V N 2004 *Phil. Mag.* B **84** 1355
[14] Ngai K L 2004 *Phil. Mag.* B **84** 1341
[15] Phillips W A, Buchenau U, Nücker N, Dianoux A-J and Petry W 1989 *Phys. Rev. Lett.* **21** 2381
[16] Yannopoulos S N and Papatheodorou G N 2000 *Phys. Rev.* B **62** 3728
[17] Boulmetis Y C, Perakis A, Raptis C, Arsova D, Vateva E, Nesheva D and Skordeva E 2004 *J. Non-Cryst. Solids* **347** 187
[18] Gurevich V L, Parshin D A and Schober H R 1998 *Phys. Rev.* B **67** 094203
[19] Taraskin S N and Elliott S R 1997 *Europhys. Lett.* **39** 37
Taraskin S N and Elliott S R 1999 *Phys. Rev.* B **59** 8572
[20] Duval E, Mermet A and Saviot L 2007 *Phys. Rev.* B **75** 024201
[21] Schirmacher W, Diezemann G and Ganter C 1998 *Phys. Rev. Lett.* **81** 136
Schmid B and Schirmacher W 2008 *Phys. Rev. Lett.* **100** 137402
[22] Benassi P, Fontana A, Frizzera W, Montagna M, Mazzacurati V and Signorelli G 1995 *Phil. Mag.* B **71** 761
[23] Elliott S R 1992 *Europhys. Lett.* **19** 201
[24] Malinovsky V K, Novikov V N and Sokolov A P 1991 *Phys. Lett.* A **153** 63
[25] Pang T 1992 *Phys. Rev.* B **45** 201
[26] Novikov V N and Sokolov A P 1991 *Solid State Commun.* **77** 243
[27] Malinovsky V K and Sokolov A P 1986 *Solid State Commun.* **57** 757
[28] Liem H, Cabanillas-Gonzalez J, Etchegoin P and Bradley D D C 2004 *J. Phys.: Condens. Matter* **16** 721
[29] Gjersing E L, Sen S and Aitken B G 2009 *J. Non-Cryst. Solids* **355** 748
[30] Boulmetis Y C, Raptis C and Arsova D 2005 *J. Optoelectr. Adv. Mater.* **7** 1209
[31] Stavrou E, Adamaki V, Sotiriou G, Kripotou S and Raptis C 2007 *J. Optoelectr. Adv. Mater.* **9** 3103
[32] Mirgorodsky A P, Merle-Méjean T, Champarnaud J-C, Thomas P and Frit B 2000 *J. Phys. Chem. Solids* **61** 501
[33] Noguera O, Merle-Méjean T, Mirgorodsky A P, Smirnov M B, Thomas P and Champarnaud-Mesjard J-C 2003 *J. Non-Cryst. Solids* **330** 50
[34] Neov S, Kozhukharov V, Gerasimova I, Krezhov K and Sidzhimov B 1979 *J. Phys. C: Solid State Phys.* **12** 2475
[35] Sekiya T, Mochida N, Ohtsuka A and Tonokawa M 1992 *J. Non-Cryst. Solids* **144** 128
[36] Sakida S, Hayakawa S and Yoko T 1999 *J. Non-Cryst. Solids* **243** 13
[37] Jaba N, Mermet A, Duval E and Champagnon B 2005 *J. Non-Cryst. Solids* **351** 833
[38] Bürger H, Vogel W and Kozhukharov V 1985 *Infrared Phys.* **25** 395

[39] Kozhukharov V, Bürger H, Neov S and Sidzhimov B 1986 *Polyhedron* **5** 771
[40] Bürger H, Kneip K, Hobert H, Vogel W, Kozhukharov V and Neov S 1992 *J. Non-Cryst. Solids* **151** 134
[41] Sekiya T, Mochida N and Ohtsuka A 1994 *J. Non-Cryst. Solids* **168** 106
[42] Duverger C, Bouazaoui M and Turrel S 1997 *J. Non-Cryst. Solids* **220** 169
[43] Ohishi Y, Mori A, Yamada M, Ono H, Nishida Y and Oikawa K 1998 *Opt. Lett.* **23** 274
[44] Naftaly M, Shen S and Jha A 2000 *Appl. Optics* **39** 4979
[45] El-Mallawany R 1998 *Mater. Chem. Phys.* **53** 93
[46] Moynihan C 1993 *J. Am. Ceramic Soc.* **76** 1081
[47] Zhu D, Ray C R, Zhou W and Day A 2003 *J. Non-Cryst. Solids* **319** 247
[48] Nukui A, Taniguchi T and Miyata M 2001 *J. Non-Cryst. Solids* **293–295** 255
[49] Hong L, Begen B, Kisliuk A, Pawlus S, Paluch M and Sokolov A P 2009 *Phys. Rev. Lett.* **102** 145502
[50] Lambson E F, Saunders G A, Bridge B and El-Mallawany R A 1984 *J. Non-Cryst. Solids* **69** 117